Posters

An EXAFS study of rare-earth phosphate glasses in the vicinity of the metaphosphate composition

R. Anderson [a,*], T. Brennan [b], G. Mountjoy [a], R.J. Newport [a], G.A. Saunders [b]

[a] *School of Physical Sciences, The University of Kent at Canterbury, Canterbury CT2 7NR, UK*
[b] *School of Physics, University of Bath, Claverton Down, Bath, BA2 7AY, UK*

Abstract

A study of rare-earth phosphate glasses, in the vicinity of the metaphosphate composition, has been undertaken at different temperatures using the extended X-ray absorption fine structure (EXAFS) facility at the Synchrotron Radiation Source, Daresbury Laboratory, UK. The metaphosphate-like glasses examined contained the rare-earth elements La, Sm, Eu and Gd as R^{3+} ions. The experiments were carried out at room temperature, 145 and 79 K. The data show that the first shell surrounding rare-earth ions contains only oxygen atoms at a mean distance of ~2.2–2.4 Å. The 'lanthanide contraction' is clearly observed, i.e., the R–O distance decreases with increasing atomic number. The observed R(–O) coordination numbers are in the range 5–7. A second correlation shell was found, associated with phosphorus atoms around the central rare-earth atom (~3.5 Å), and another rare-earth:oxygen correlation was also identified (~4 Å). Static disorder dominates the Debye–Waller term, but thermal disorder is not negligible. Within the accuracy of the EXAFS data, no significant structural variations were observed over the temperature range studied. We conclude that the anomalous bulk properties are associated with either subtle structural features or primarily due to rare-earth ion interactions. © 1998 Elsevier Science B.V. All rights reserved.

1. Introduction

Glasses containing rare-earth ions have great importance in the laser and optoelectronics industry. In the majority of the glasses, the rare-earth modifier concentration is at low dopant levels. However, with the rare-earth metaphosphate glasses, having a composition near $(R_2O_3)_{0.25}$ $(P_2O_5)_{0.75}$, dopant levels are significantly larger, and become strongly magnetic at low temperatures [1].

Rare-earth metaphosphate glasses are known to possess unusual properties. For example, europi-um and samarium metaphosphate glasses show pronounced acoustic mode softening with increase of pressure or decrease of temperature: the hydrostatic pressure derivatives $(\partial C_{11}/\partial P)_{T,P=0}$ and $(\partial C_{44}/\partial P)_{T,P=0}$, and also the bulk modulus $(\partial B/\partial P)_{T,P=0}$ are negative, i.e., as pressure is applied the glass becomes easier to squeeze [2,3]. Furthermore as the temperature is reduced to 77 K, for europium metaphosphate the negative values of $(\partial C_{11}/\partial P)_{T,P=0}$ and $(\partial B/\partial P)_{T,P=0}$ become larger [2]. In complete contrast other rare-earth phosphate glasses have positive values for these properties, (e.g., in lanthanum metaphosphate, the elastic stiffness increases in the more usual way as temperature falls [3]). Those REMGs, which have soft acoustic modes, also have negative thermal expansion coefficients [4].

* Corresponding author. Tel.: +44 1227 764000/3776; fax: +44 1227 827558; e-mail: raz@ukc.ac.uk.

X-ray diffraction studies of the atomic-scale structure of these glasses have confirmed that the basic network is made up of PO_4 tetrahedra [5,6]. The extended X-ray absorption fine structure (EXAFS) work [7] established that the rare-earth ions are surrounded by 6–8 oxygen atoms on average at a distance of approximately 2.25–2.40 Å, depending on the rare-earth ion. A correlation between the rare-earth and phosphorus atoms was also found between 2.7–3.6 Å and a second rare-earth–oxygen correlation at ~4 Å [7].

Given that the glasses display unusual acoustic and thermal properties at low temperatures (below ~100 K), a study was needed to compare the structures between room temperature and liquid nitrogen temperatures. EXAFS was used to probe the local environment of the rare-earth ion in the glass. This was carried out using the L_{III} absorption associated with the rare-earths, La, Sm, Eu and Gd.

2. Experimental

The rare-earth phosphate glasses were made following to the procedure outlined in Ref. [8]. The chemical compositions of the samples studied were measured using electron probe micro-analysis and are given in Table 1.

The glass samples were crushed between steel plates and then ground to a fine powder (~1 μm) using an agate mortar and pestle. The powder was dusted on to adhesive tape with a number of such layers being used for each experiment to help ensure a uniform optical thickness in the X-ray beam and that the ratio of the absorption edge to the background was approximately 0.5–1.5 so that good experimental statistics could be obtained. The EXAFS data were collected in transmission mode; room temperature data were

collected with the samples mounted directly in the beam line, and a variable temperature cryostat was used for experiments at 145 and 79 K.

The EXAFS experiment was carried out using stations 7.1 and 8.1 at the SRS, Daresbury Laboratory, UK. The energy ranges available for EXAFS studies are 4–12 and 3.5–11 keV for stations 7.1 and 8.1, respectively, i.e. covering the energy range of the rare-earth L_{III} edges. The k range of the EXAFS spectra was limited, however, by the presence f the L_{II} absorption edges; this resulted in having to truncate the measured spectrum and hence reducing the resolution in real space. The k range accessible was approximately 2 to 10–12 Å^{-1}.

3. Theory and analysis

EXAFS spectroscopy is a method for obtaining direct information on the short range structural environment of an specific atom type in a material. A simplified, heuristic, equation describing the EXAFS spectrum (using plane wave theory) [9] is given below in order to illustrate the salient features.

$$\chi(k) = S(k)\{\sin(2kR + 2\delta + \varphi)$$
$$\exp(-2R/\lambda)\exp(-2\sigma^2 k^2)\}, \qquad (1)$$

where S depends on the number of back-scattering atoms and an amplitude factor, k is the wave vector of the photoelectron, R is the distance between excited atom and neighbouring back-scattering atom, δ and φ are the phase shifts induced in the electron wave by the excited atom and the back-scattering atom potentials (respectively), λ is the mean free path of the photoelectron and σ is the exponent in the Debye–Waller term, which accounts for static and thermal disorder in the structure. Note, the definition of k in

Table 1
Compositions of glasses studied

Rare-earth element	Atomic number	Composition of glass (± 0.005)
Lanthanum	57	$(La_2O_3)_{0.1999}(Gd_2O_3)_{0.0001}(P_2O_5)_{0.8000}$
Samarium	62	$(Sm_2O_3)_{0.224}(P_2O_5)_{0.776}$
Europium	63	$(Eu_2O_3)_{0.218}(P_2O_5)_{0.782}$
Gadolinium	64	$(Gd_2O_3)_{0.229}(P_2O_5)_{0.771}$

EXAFS back-scattering formalism is such that it is a factor two smaller than the analogous diffraction case.

Data analysis was carried out using EXCALIB, EXBACK and EXCURV92, the suite of programs at the Daresbury Laboratory. EXCALIB is used to sum the multiple sets of data, EXBACK is used for background subtraction and normalising the spectrum and EXCURV92 is used to fit to the EXAFS spectrum via fast curved wave theory [10,11]. The more conventional approach to data analysis assumes Gaussian distributions of atomic separations, which may not be appropriate for a glass, hence a cumulant expansion approach to the EXAFS data analysis was also used. Eq. (1) is modified to become

$$\chi(k) = S(k)\{ \sin(2kR + 2\delta + \varphi - \tfrac{4}{3}(kC_3)^3)$$
$$\exp(-2R/\lambda)\exp(-2\sigma^2 k^2 + \tfrac{2}{3}(kC_4)^4)\}, \quad (2)$$

where C_3 and C_4 are the third and fourth cumulants, respectively, and these factors are taken into account during the iteration of parameters in the EXCURV92 analysis.

Calibration of the EXAFS spectra and verification of the suitability of EXCURV92's rare-earth phase shifts were achieved by using data collected for crystalline neodymium ultraphosphate (NdP_5O_{14}) at a temperature of 105 K. It was thereby also confirmed that the amplitude factor (present in the full EXAFS equation) was approximately 0.7, which is consistent with previous work [7]. This value was used in the data analysis using

Table 2
Summary of EXAFS results from spectra for the rare-earth phosphate glasses in the vicinity of the metaphosphate composition, where R represents the rare-earth ion

Glass	Correlation	Coordination	Distance (Å)	$2\sigma^2$ (Å^2)	Temperature (K ($\pm$5))
La	R–O	7.3 ± 1.2	2.42 ± 0.03 [a]	0.030 ± 0.012	293
	R–P	5.9 ± 4.4	3.54 ± 0.04	0.042 ± 0.046	
La	R–O	6.0 ± 0.6	2.42 ± 0.02 [a]	0.017 ± 0.005	145
	R–P	3.0 ± 1.5	3.60 ± 0.03	0.017 ± 0.019	
La	R–O	5.9 ± 0.4	2.41 ± 0.02 [a]	0.013 ± 0.004	79
	R–P	3.6 ± 2.1	3.61 ± 0.04	0.028 ± 0.030	
Sm	R–O	6.9 ± 0.3	2.31 ± 0.01	0.019 ± 0.002	293
	R–P	16.3 ± 7.1	3.40 ± 0.02	0.124 ± 0.037	
	R–(P–)O		4.03 ± 0.01		
Sm	R–O	6.4 ± 0.3	2.33 ± 0.01	0.016 ± 0.002	145
	R–P	5.7 ± 9.1	3.41 ± 0.05	0.071 ± 0.063	
	R–(P–)O		4.07 ± 0.02		
Sm	R–O	6.9 ± 0.9	2.32 ± 0.01	0.013 ± 0.005	79
	R–P	10.8 ± 13.4	3.41 ± 0.05	0.095 ± 0.067	
	R–(P–)O		4.08 ± 0.01		
Eu	R–O	6.2 ± 0.3	2.31 ± 0.01	0.016 ± 0.002	293
	R–P	5.0 ± 4.1	3.34 ± 0.05	0.082 ± 0.055	
	R–(P–)O		4.07 ± 0.02		
Eu	R–O	6.0 ± 0.3	2.32 ± 0.01	0.012 ± 0.002	145
	R–P	3.9 ± 3.4	3.33 ± 0.05	0.072 ± 0.052	
	R–(P–)O		4.03 ± 0.02		
Eu	R–O	6.0 ± 0.3	2.30 ± 0.01	0.012 ± 0.002	79
	R–P	4.0 ± 3.7	3.34 ± 0.05	0.074 ± 0.056	
	R–(P–)O		4.04 ± 0.02		
Gd	R–O	5.0 ± 0.4	2.28 ± 0.01	0.014 ± 0.003	293
Gd	R–O	5.0 ± 0.3	2.27 ± 0.01	0.008 ± 0.002	145
Gd	R–O	5.0 ± 0.4	2.27 ± 0.01	0.008 ± 0.002	79

[a] Obtained using Fourier filtering.

EXCURV92, which assumes that the chemical environment of the rare-earth ions in the metaphosphate-like glass samples is similar to that of the Nd^{3+} ion in the crystalline ultraphosphate.

It is observed that an anomalous feature appeared in the spectra obtained for the lanthanum metaphosphate-like glass. This occurred between $k = 5.5$ and 6.5 $Å^{-1}$ and is similar to features observed in earlier work [7]. It is possible that this feature is due to effects of double electron peaks in the EXAFS spectrum [7], which give unphysically low interatomic distances in the Fourier transform. Fourier filtering methods were used to establish the effect of the anomaly, with the filtering window covering the range $R = 1.5$–4.0 Å, such that both unphysical and 'noise-dominated' real-space features are eliminated. The feature was virtually removed from the k-space back-transform and we therefore conclude that it was indeed anomalous. For the analysis of lanthanum phosphate, the data points associated with the feature were deleted. It was also necessary to remove other data points in some files, since 'glitches' occurred, due to imperfections in the monochromator. This is a normal procedure when using EXCURV92 to fit EXAFS data [12].

4. Results

The results obtained from fitting the EXAFS spectra are summarised in Table 2. As an example, the EXAFS spectrum and the associated Fourier transform for Eu phosphate glass at a temperature of 145 K are shown in Figs. 1 and 2. All results shown are those obtained using the cumulant fit in the analysis. The uncertainties quoted in the table are those obtained by using the variation of fit index to generate a goodness-of-fit map for pairs of correlated fit parameters. Of importance then is the correlation between the Debye–Waller factor and the number of neighbouring atoms and the analogous correlation between distances and the effective position of the EXAFS E_f (the energy difference between vacuum and the edge being examined). Fig. 3 shows an example of this. The minimum fit index is displayed in the plot and also a bold contour corresponding to twice the
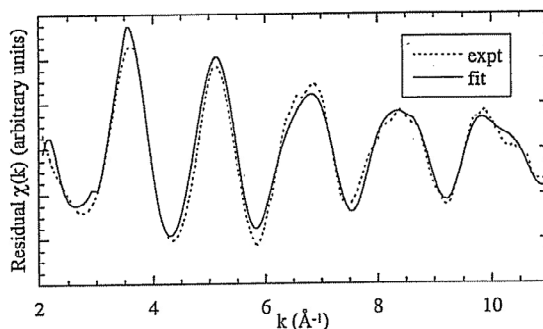

Fig. 1. EXAFS $\chi(k)$ for europium phosphate glass in the vicinity of the metaphosphate composition at 145 K, experimental data (dotted line) and theoretical fit (solid line).
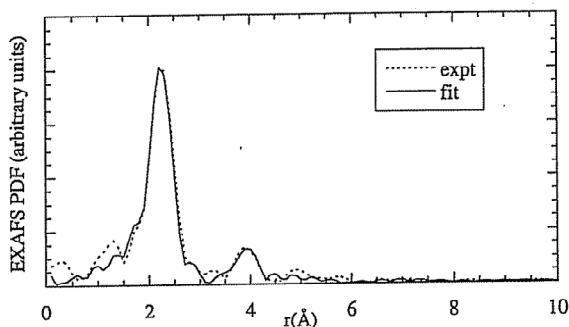

Fig. 2. EXAFS pair distribution function for europium phosphate glass in the vicinity of the metaphosphate composition at 145 K, experimental data (dotted line) and theoretical fit (solid line).

standard deviation – it is the extent of this uncertainty ellipse that is taken as the error value.

5. Discussion

The lanthanide contraction is clearly seen as a reduction in the first shell rare-earth–oxygen distance with increasing atomic number. This is shown in Fig. 4. No rare earth – rare earth correlations were found in the data obtained; within the limits of our data it is therefore possible to state that there is no clustering of the rare-earth (R) ions ~4 Å. For a random distribution, the average R–R distance is expected to be between 4 and 6 Å. As expected, the Debye–Waller factors for this first coordination shell are seen to increase as temperature
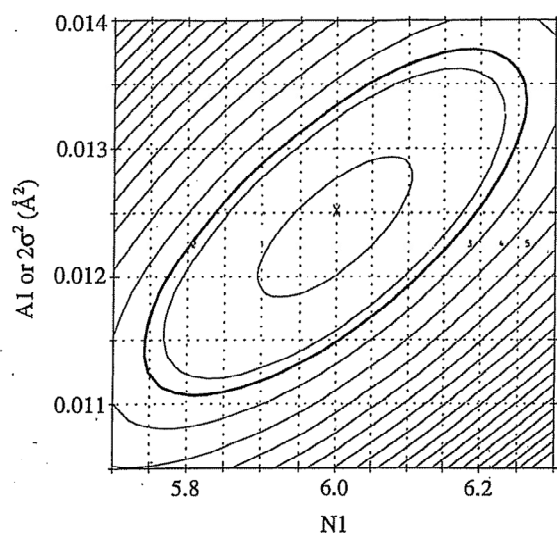
Fig. 3. Correlation map for europium phosphate glass in the vicinity of the metaphosphate composition at 145 K showing goodness of the fit for the parameters N1 (number of neighbouring oxygen atoms in the first shell) and A1 (Debye–Waller factor, $2\sigma^2$, for the first shell).

Fig. 5. Rare-earth–oxygen coordination number variation with atomic number of the metaphosphate-like glasses. Symbols O represents 293 K, × represents 145 K, and □ represents 79 K.

increases for each of the glasses. This indicates significant thermal disorder relative to the dominant static disorder.

The variation of first shell coordination number with atomic number of the rare-earth element is shown in Fig. 5. The first shell coordination numbers vary between 5 and 7. These are somewhat
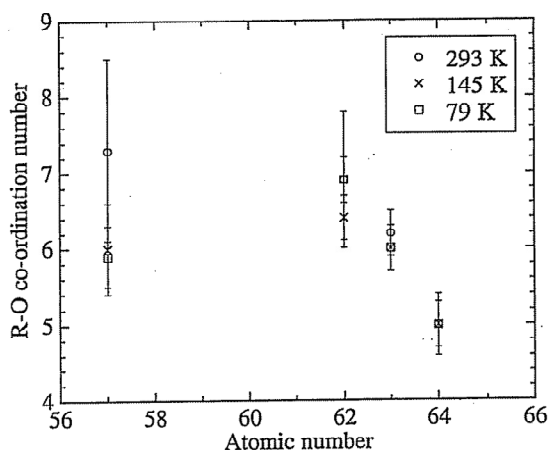
lower than measured in previous work which suggested values lying between 6 and 8 [5,7]. (The difference may be due to our modified method in fitting to the data.) It is important to consider the correlation between rare-earth ion size and the first shell (oxygen) coordination number. In the crystalline analogues [13–15] the oxygen coordination number decreases from 8 to 6 as ion size decreases. Such a trend could be consistent with the results shown in Fig. 5, and would indicate significant short-range structural similarities.
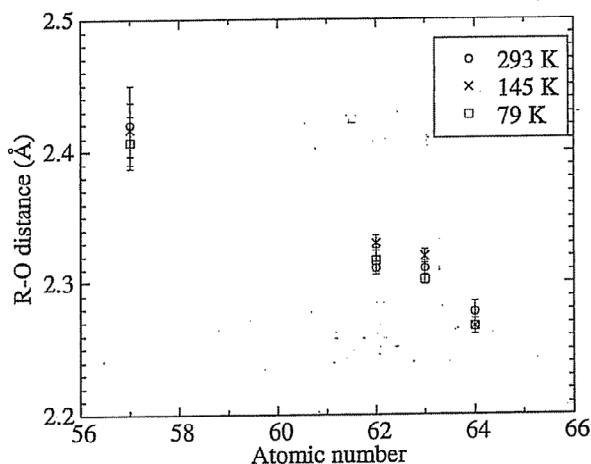

Fig. 4. Rare-earth–oxygen distance variation with atomic number of the metaphosphate-like glasses, demonstrating the lanthanide contraction. Symbols O represents 293 K, × represents 145 K, and □ represents 79 K.

Fig. 5 also appears to show a marked decrease in the rare-earth oxygen coordination number between Sm and Gd phosphate samples. Unfortunately, it is not possible to conclude that these effects are definitely occurring, for the following reasons.

The uncertainties in coordination number are quite large (in particular for La phosphate). In addition, it must be considered that N_{RO} may depend on the rare-earth content, because the amount of non-bridging oxygen atoms relative to rare-earth ions increases for rare-earth oxide content less than 25 mol%. For the samples presented here, the La phosphate has the lowest rare-earth content and Gd phosphate has the highest rare-earth content. This might tend to increase and decrease N_{RO}, respectively, as suggested by the data in Fig. 5. However, it should also be noted that the data in Fig. 5 could be consistent with an approximately constant R–O coordination number of 6. In fact, the R–O distances obtained in this study are all close to those calculated for $N_{RO} = 6$, rather than $N_{RO} = 8$ [16].

The measured EXAFS spectra were fitted with a second shell, associated with a rare-earth–phosphorus correlation between approximately 3.3 and 3.6 Å (except for the gadolinium phosphate data, which did not show this correlation). The data for europium and samarium phosphate is of sufficient quality that a third shell, of oxygen, is found at ~4 Å. Such R–P second shells and a R(–P)–O third shells are expected based on the metaphosphate crystal structures. The observed coordination numbers for the R–P shell are generally consistent with the expected values of 6, considering the large uncertainties. Fitting to a third shell in general can give reliable distances, but not coordination numbers. This is the reason that R–O distance for the third shell is given in Table 2, but coordination number and associated Debye–Waller factor are not. The observed distance of ~4 Å is consistent with the beginning of the R(–P)–O correlation in the metaphosphate crystal structures. Therefore, the present results are consistent with rare earth ions coordinated to non-bridging oxygens of the surrounding phosphate network, in a similar manner to that seen in the analogous crystal structures.

No significant change is observed between the results obtained at the different temperatures. This indicates very clearly that, within the errors and limitations of our data, any structural changes associated with the observed temperature dependent changes in bulk properties are subtle. Indeed, the evidence suggested that a structural explanation is not likely to reside in the first (R–O) or second (R–P) coordination shells. The use of computer modelling methods, employing rare-earth-sensitive X-ray data together with high real-space resolution neutron diffraction results, may offer a way forward in this regard.

6. Conclusions

The present study of the rare-earth environment in a series of new rare-earth phosphate glasses, in the vicinity of the metaphosphate composition, has
1. confirmed the anticipated fact that the rare earth ions have a local environment similar to that in metaphosphate crystal structures;
2. shown the expected lanthanide contraction;
3. shown that within the limitations of the data, there is not a structural origin at the first shell level of the temperature dependence of bulk properties;
4. shown that the rare-earth ions are separated by distances greater than ~4 Å in the glass i.e., there is no clustering at shorter distances.

Acknowledgements

References

[1] P.J. Ford, C.D. Graham, G.A. Saunders, H.B. Senin, J.R. Cooper, J. Mater. Sci. Lett. 13 (1994) 697.

[2] H.M. Farok, H.B. Senin, G.A. Saunders, W. Poon, H. Vass, J. Mater. Sci. 29 (1994) 2847.

[3] H.A.A. Sidek, G.A. Saunders, R.N. Hampton, R.C.J. Draper, B. Bridge, Philos. Mag. Lett. 57 (1988) 49.

[4] M. Acet, T. Brennan, M. Cankurtaran, G.A. Saunders, to be published.

[5] D.T. Bowron, R.J. Newport, B.D. Rainford, G.A. Saunders, H.B. Senin, Phys. Rev. B 51 (1995) 5739.

[6] D.T. Bowron, G. Bushnell-Wye, R.J. Newport, B.D. Rainford, G.A. Saunders, J. Phys.: Condens. Matter 8 (1996) 3337.

[7] D.T. Bowron, G.A. Saunders, R.J. Newport, B.D. Rainford, H.B. Senin, Phys. Rev. B 53 (1996) 5268.

[8] A. Mierzejewski, G.A. Saunders, H.A.A. Sidek, B. Bridge, J. Non-Cryst. Solids 104 (1988) 323.

[9] E.A. Stern, in: D.C. Koningsberger, R. Prins (Eds.), X-ray Absorption. Principles, Applications, Techniques of EXAFS, SEXAFS and XANES, Wiley, New York, 1988.

[10] S.J. Gurman, N. Binsted, I. Ross, J. Phys. C: Solid State Phys. 17 (1984) 143.

[11] S.J. Gurman, N. Binsted, I. Ross, J. Phys. C: Solid State Phys. 19 (1986) 1845.

[12] J.F.W. Mosselmans, Daresbury Laboratory, UK, private communication.

[13] H.Y.-P. Hong, Acta Crystallogr. B 30 (1974) 468.

[14] H.Y.-P. Hong, Acta Crystallogr. B 30 (1974) 1857.

[15] J. Matuszewski, J. Kropiwnicka, T. Znamierowska, J. Solid State Chem. 75 (1988) 285.

[16] R.D. Shannon, Acta Crystallogr. A 32 (1976) 751.